J. DIFERENSIAL/E-ISSN:2775-9644
Vol.6(2),2024, 148–169
doi:https://doi.org/10.35508/jd.v6i2.17868

RESEARCH ARTICLE

Mathematical (Seirb) Model Analysis for Evaluating Cholera Control Strategies in Remote Dry Season Region

Zainab Olabisi Dere[1,*], Asimiyu Olalekan Oladapo[2]

[1]*Florida State University, USA*
[2]*Osun State University, Osogbo, Nigeria*
[*]*Corresponding author: zod20@fsu.edu*

Received: 28 July 2024; Revised: 8 September 2024; Accepted: 18 September 2024; Published:1 November 2024.

Abstract:
Cholera, caused by the Vibrio cholerae bacterium, poses a significant public health threat in remote regions of Nigeria, especially during the dry season when access to treated water is limited. This research aims to develop a comprehensive model to understand the rapid spread of cholera in these areas and evaluate the efficacy of control policies, including educational programs, antibiotics, water treatment rates, and environmental cleanliness through resolving the Existence and Uniqueness of the model formulation, Positivity, and Boundedness, Basic Reproduction Number, R_0 i.e. the threshold of the disease dynamics. When $R_0 < 1$ the versatility of the disease spreads will die out with time and if $R_0 > 1$, the persistence of the disease prevails over time. Local and Global stability analysis of the model was obtained, also the sensitivity analysis for the targeted parameters was analyzed. Additionally, the study incorporates numerical simulations utilizing the homotopy perturbation method to identify the specific impact of the control parameters are for in mitigating the spread of the Vibrio cholerae disease. The result obtained seeks to provide valuable insights into designing effective intervention strategies aforementioned to combat cholera outbreaks in resource-constrained regions, with a focus on improving water accessibility and implementation.

Keywords: Cholera, Basic Reproduction Number, Stability Analysis, Treatment Rate, Homotopy Perturbation Method

1. Introduction

Cholera is a severe disease transmitted primarily through the fecal-oral route, often due to contaminated water and inadequate sanitation [1]. The bacterium *Vibrio cholerae* causes cholera and thrives in poor hygiene environments, leading to severe diarrhea and dehydration that can be fatal if untreated. Cholera outbreaks place immense pressure on healthcare systems, increase mortality rates, and strain medical resources, especially in vulnerable populations like children and the elderly [2, 3]. In Northern Nigeria, where cholera remains a persistent public health challenge, factors such as arid climate, limited access to clean water, and inadequate sanitation exacerbate the spread of the disease. This region's geography, socio-economic conditions, and the dry season's environmental factors create favorable conditions for the proliferation of vibrio cholerae, making cholera control

efforts particularly challenging [4, 5]. In order to understand and predict cholera outbreaks and devise appropriate intervention strategies, it is critical to develop models that accurately represent the dynamics of cholera transmission. The Susceptible, Vaccinated, Exposed, Infected, Recovered, and Bacteria (SVEIRB) model offers a robust mathematical framework for studying the transmission of cholera in environments such as Northern Nigeria. This model incorporates key epidemiological factors such as the spread of bacteria, the immunity level of the population, and environmental conditions that influence bacterial persistence, including the environmental bacteria coefficient (c) [6].

Cholera transmission is driven by the interaction between humans and the environment, particularly through contact with contaminated water sources. Vibrio cholerae thrives in contaminated water, especially in regions with inadequate sanitation and clean water access, as seen in Northern Nigeria during the dry season. The transmission dynamics of cholera can be divided into two main components: human-to-human transmission through fecal-oral routes and environmental transmission through exposure to contaminated water [7–9]. The Human-to-Human Transmission occurs when individuals ingest food or water contaminated with the cholera bacteria. In areas with poor hygiene, the bacteria spread rapidly from infected individuals to healthy people through shared water sources or contaminated food [10, 11]. The environmental transmission persist in water bodies, especially when they are poorly treated or stagnant, as is common in regions facing water scarcity. During dry seasons in Northern Nigeria, water scarcity becomes more pronounced, forcing communities to rely on contaminated water sources for drinking, cooking, and irrigation [12]. This creates a cyclical pattern of bacterial contamination and human exposure, driving the persistence and spread of cholera [13]. A crucial factor in the environmental transmission of cholera is the environmental bacteria coefficient (c), which represents the rate at which bacteria proliferate in the environment. This coefficient is influenced by several factors, including temperature, water quality, and the availability of nutrients for the bacteria [14]. In arid regions such as Northern Nigeria, where water quality deteriorates during the dry season, the environmental bacteria coefficient increases, leading to more rapid bacterial growth and a higher likelihood of outbreaks [15–17]. Immunity Levels of the Population: Northerners and Their Vulnerability Immunity plays a significant role in determining the susceptibility of a population to cholera. In Northern Nigeria, the immunity levels of the population vary widely due to factors such as previous exposure to cholera, vaccination coverage, and overall health conditions [16, 18, 19]. This model accounts for these variations by categorizing individuals into different compartments: susceptible (S), vaccinated (V), exposed (E), infected (I), recovered (R), and the bacterial environment (B) [20].

This compartment includes individuals who have not been exposed to cholera and have no immunity to the disease. These individuals are at the highest risk of infection, particularly during outbreaks, and Vaccinated consists of individuals who have received a cholera vaccine, providing them with some level of protection against the disease. Vaccination is a crucial component of cholera control strategies, particularly in regions with recurring outbreaks [21]. An exposed individuals in this compartment have been exposed to *Vibrio cholerae* but are not yet symptomatic. They may develop the disease after the incubation period or recover without developing symptoms, depending on their immune response [22]. More so, infected individuals includes individuals who are actively infected and capable of transmitting the disease to others, either through direct contact or by contaminating water sources while recovered Individuals in this category have survived cholera and gained immunity, either temporarily or permanently, depending on the strain of cholera and their overall health [23]. Hence, bacteria contracted individuals represents the environmental reservoir of cholera, including contaminated water bodies where the bacteria can persist and spread to humans [24].The model's ability to capture these different population dynamics is crucial for understanding how cholera spreads and persists in Northern Nigeria, particularly given the population's varied immunity levels. Immunity can be influenced by several factors, including age, nutrition, and access to

healthcare. Children, the elderly, and those with weakened immune systems are particularly vulnerable to severe cholera infections [25].Environmental Bacteria Coefficient (c) and Its Impact on Cholera Transmission. The environmental bacteria coefficient (c) is a critical parameter in the SVEIRB model, as it directly influences the rate at which *Vibrio cholerae* proliferates in water sources. This coefficient is affected by several environmental factors, including temperature, nutrient availability, and the presence of contaminants that may support bacterial growth [26]. In Northern Nigeria, the dry season creates conditions that are particularly conducive to bacterial growth. Water scarcity forces communities to rely on unsafe water sources, which are often contaminated with human waste due to inadequate sanitation infrastructure. The environmental bacteria coefficient (c) increases as water quality deteriorates, leading to more rapid bacterial proliferation and a higher risk of cholera transmission [27]. This relationship between water quality and the environmental bacteria coefficient is central to understanding the seasonal dynamics of cholera outbreaks in Northern Nigeria [28]. The model can be expressed mathematically through a system of differential equations that describe the rates of change between the different compartments (S, V, E, I, R, and B). These equations take into account the transmission rates, recovery rates, and environmental factors that influence the spread of cholera. One of the challenges in developing the SVEIRB model is accurately estimating the parameters that influence cholera transmission. These parameters, including the environmental bacteria coefficient (c), transmission rates, and recovery rates, vary depending on local conditions such as climate, sanitation infrastructure, and population density [29]. In Northern Nigeria, where water scarcity and poor sanitation are pervasive, the environmental factors

Cholera is a severe disease transmitted primarily through the fecal-oral route, often due to contaminated water and inadequate sanitation [1]. The bacterium Vibrio cholerae causes cholera and thrives in poor hygiene environments, leading to severe diarrhea and dehydration that can be fatal if untreated. Vulnerable populations, such as children and the elderly, are particularly at risk [2]. The cholera outbreaks strain healthcare systems, increasing mortality rates and burdening medical resources [3]. Northern Nigeria is especially vulnerable to cholera due to its arid climate and limited access to clean water, particularly during the dry season. Water scarcity leads to more contaminated water sources, creating ideal conditions for Vibrio cholerae to spread [4, 5]. The region's health infrastructure struggles to cope with surges in cholera cases, worsening health outcomes [6]. It also have significant economic impacts. Increased healthcare costs strain public health budgets, and the loss of productivity due to illness disrupts economic activities [7]. The tourism industry may suffer, and foreign investment can be deterred by poor health conditions. In northern Nigeria requires improved sanitation, access to clean water, and stronger healthcare systems [8]. Public awareness on hygiene and early detection is crucial. International cooperation is essential for building resilience and mitigating the economic impacts of cholera outbreaks. Developing effective cholera control strategies in northern Nigeria is imperative [9–12]. This involves understanding the dynamics of cholera transmission in remote areas during the dry season, where water scarcity and contaminated water sources heighten the risk [14]. A comprehensive model capturing these dynamics, along with existing control policies such as education, antibiotics, water treatment, and environmental cleanliness, is necessary [13, 15, 16]. Numerical simulations, such as the homotopy perturbation method, can optimize control parameters and identify effective interventions [17]. Farm practices, drought, and contaminated water consumption compound cholera challenges during the dry season [18, 19, 22]. Water scarcity forces communities to use contaminated water for irrigation, creating a cycle of disease transmission. Persistent drought exacerbates water scarcity, compromising hygiene and increasing the risk of waterborne diseases like cholera [20, 21]. Communities often rely on unsafe water sources, inadvertently spreading Vibrio cholerae [23]. The complex interplay of farming practices, drought, and contaminated water consumption is crucial for addressing cholera in northern Nigeria . This understanding can inform targeted and effective control measures. The goal is to empower communities with the knowledge and tools to break the cholera cycle and build resilience [24]. The

findings aim to inform policy development, public health initiatives, and community interventions, fostering a cholera-resistant population in these vulnerable regions. However, the need for a multi-faceted approach that includes improved sanitation, clean water access, robust healthcare systems, public awareness, and international cooperation, the strategy aims to mitigate the impacts of cholera [25, 26]. Moreover, the use of numerical simulations to optimize control strategies can help in developing effective interventions tailored to the unique challenges of northern Nigeria [27]. Through comprehensive measures addressing both immediate and long-term needs, the goal is to reduce the incidence of cholera and improve the overall health and resilience of the affected communities.

2. Mathematical Formulation

A total population N(t) is considered which is divided into sub-populations of S of susceptible population, E(t) exposed , I(t) infected, R(t) recovered population and B(t) bacteria causing population . The level of individuals migrating into the population at Λ, effective contact rate of an individual τ and the level of the spread induced rate at δ. Transmission rate in cholera disease between the two or more population of individuals being exposed at β . The modification of the disease capacity multiplicative effect is at a rate c, and enlightenment through educational program initiatives on the rapid spread on how deadly cholera is is at a rate of ω. Prevention on the spread with a waning rate η and regular treatment of cholera disease with antibiotics is at rate of ε. An infected individual are subjected to recover at a rate of r and individuals that are hospitalized having been infected is $(1-\varepsilon)$ while that of infected are said to recover at a rate of $(r+\varepsilon)$. Moreso, set of bacteria individual form back into the susceptible population through water treatment occurs at at rate of T when immunity level is high. Respective individuals across the sub-population are subjected to death naturally by μ. Pictorial illustration of this can be displayed from the figure below

2.1. Existing Model

A proposed compartmental-based model for analyzing the dynamics of the spread of cholera transmission disease. The governing model is given by the system of non-linear ordinary differential equations below:

$$\begin{aligned}
\frac{dS}{dt} &= \mu N - \beta_1(I,t)SI - \beta_2(B,t)\frac{SB}{\kappa + B} - \mu S \\
\frac{dI}{dt} &= \beta_1(I,t)SI - \beta_2(B,t)\frac{SB}{\kappa + B} - (\gamma + \mu)I \\
\frac{dR}{dt} &= \gamma I - \mu R \\
\frac{dB}{dt} &= rB\left(1 - \frac{B}{K}\right) + \xi I - \delta(t)B
\end{aligned}$$

N is the total population as $S(0) = s_o, I(0) = i_o, R(0) = r_o, B(0) = b_o \quad \geq 0.$

2.2. The Modified Model

The modeified was extended by incorporating educational program ω, water treatment rate with antibiotics T and environmental bacteria cleanliness c the recovery rate.The model equation is as

follows.

$$\begin{aligned}
\frac{dS}{dt} &= \Lambda - \beta S(t)I(t) - (\tau + \omega)S(t) + TB(t) - \mu S(t) \\
\frac{dE}{dt} &= \beta S(t)I(t) - (c + \eta + \mu)E(t) \\
\frac{dI}{dt} &= \tau S(t) + (c + \eta)E(t) - (\varepsilon + \delta + r + \mu)I(t) \\
\frac{dR}{dt} &= \omega S(t) + (r + \varepsilon)I(t) - \mu R(t) \\
\frac{dB}{dt} &= -(T + \mu)B(t)
\end{aligned} \tag{2.1}$$

By initial condition that $0 \leq T \leq 1$. When $T = 0$, vulnerable individuals are not immunized or immunization does not affect the vulnerable compartment.

2.3. Tables and Figures

Table below depicts description of respective parameters, values and references.

Table 2.1: Description of the parameters and values

Parameter	Description	Values	Units	Refs.
N	Total population	70000		
S	Susceptible population of children	42500		
E	Exposed population	2050		
I	Infected population	1042		
R	Recovered population	21485		
B	Vibro Cholerae (Parasite) population	2923	per day^{-1}	[12]
Λ	Recruitment rate into the susceptible population	0.012	per day^{-1}	[5, 8]
τ	Vibro Cholerea multiplicative effect	0.31	per day^{-1}	[19]
T	Water treatment rate on rapid vibro intrinsic growth rate	0.011	per day^{-1}	[20–23]
μ	Natural death from the population	0.01	per day^{-1}	[18]
ω	Rate of educational program	0.2102	per day^{-1}	[1, 7, 15]
β	Transmission Coefficient	0.1	per day^{-1}	[13]
η	Wanning rate of immunity	0.2317	per day^{-1}	[2]
c	Environmental bacteria capacity	0.31	Assumed (per day^{-1})	[7, 18]
ε	Treatment rate with antibiotics	0.815	per day^{-1}	[17]
δ	Rate of induced death	0.3	per day^{-1}	[10, 16]
r	Recovery rate from infected population	1.7601	per day^{-1}	[12, 19]

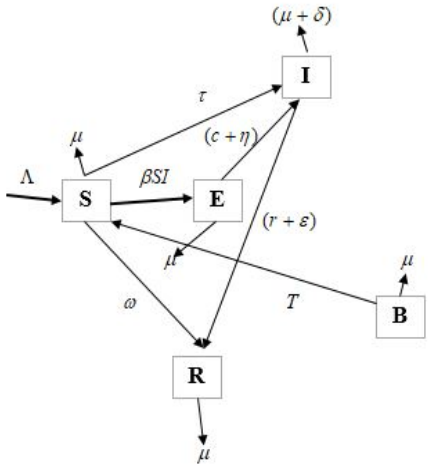

Figure 2.1: The Schematic flow of the SEIRB Model

3. Model Analysis

3.1. Existence and Uniqueness of the Model

Examining the population-related segment of the system of equations, we have
$N(t) = S(t) + E(t) + I(t) + R(t) + B(t)$
The derivatives obtained as,

$$\frac{dN(t)}{dt} = \frac{d}{dt}\Big(S(t),, E(t), I(t), R(t), B(t)\Big)$$

$$\frac{dN(t)}{dt} = \frac{dS}{dt} + \frac{dE}{dt} + \frac{dI}{dt} + \frac{dR}{dt} + \frac{dB}{dt}$$

$$\frac{dN(t)}{dt} = \Big\{(\Lambda - \beta S(t)I(t) - (\tau+\omega)S(t) + TB(t) - \mu S(t)) + (\beta S(t)I(t) - (c+\eta+\mu)E(t))$$

$$+ (\tau S(t) + (c+\eta)E(t) - (\varepsilon+\delta+r+\mu)I(t)) + (\omega S(t) + (r+\varepsilon)I(t) - \mu R(t)) + (-(T+\mu)B(t))\Big\}$$

$\frac{dN(t)}{dt} \leq \Lambda - \mu N - \delta I(t)$ where no outbreak of cholera is observed, $\delta = 0$

$\frac{dN}{dt} + \mu N \leq \Lambda$

$N(t)e^{\mu t} = \frac{\Lambda e^{\mu t}}{\mu} + C$, as where c is a constant of integration

$N(t) = \frac{\Lambda}{\mu} + Ce^{-\mu t}$

By the initial condition at $t = 0$
$C = N(t) - \frac{\Lambda}{\mu} \quad C = N(0) - \frac{\Lambda}{\mu}$
As time progresses, N(t) is such that;

$$\lim_{t\to\infty} N(t) \leq \lim_{t\to\infty}\left[\frac{\Lambda}{\mu} + \left(N(0) - \frac{\Lambda}{\mu}\right)e^{-\mu t}\right] = \frac{\Lambda}{\mu}$$

If $N(0) \leq \frac{\Lambda}{\mu}$, then $N(t) \leq \frac{\Lambda}{\mu}$. Thus, $\Re_+^5$ is a positive invariant set under the flow described by 3.2 so that no solution path leaves through any boundary of $\Re_+^5$. Hence, it is sufficient to consider the dynamics of the model in the domain $\Re_+^5$. In this region, the model can be considered to be mathematically and epidemically well-posed representing a physical problem. This shows that the total population N(t), i.e., the sub-population S(t), E(t), I(t), R(t), and B(t) of the model are bounded and is a unique solution. Hence, it represents a physical problem.

3.2. Positivity and Boundedness of the Model Solution

Theorem 1

Let x, y be distinct points of a normed linear space $(X, \| \cdots \|)$ over $\Re$. Then the map $f : [0,1] \subseteq \Re \to (X, \| \cdot \|)$, such that $f(\lambda) = \lambda x + (1-\lambda)y$ is continuous on $[0,1]$

Proof :

Let $\lambda_0 \in [0,1]$. then $f(\lambda_0) = \lambda_0 x + (1-\lambda_0)y$ for any $\lambda \in [0,1]$,

$$\begin{aligned} \| f(\lambda) - f(\lambda_0) \| &= \| (\lambda - \lambda_0)x + (\lambda_0 - \lambda)y \| \\ &\leq | \lambda - \lambda_0 | (\| x \| + \| y \|). \end{aligned}$$

If $\varepsilon > 0$ is given, let $\delta = \frac{\varepsilon}{\|x\|+\|y\|}$. If $| \lambda - \lambda_0 | < \delta$, then the $\| f(\lambda) - f(\lambda_0) \| < \varepsilon$, . Therefore, f is continuous at λ_0. Since λ_0 is an arbitrary point in $[0,1]$, then f is continuous on $[0,1]$. Let X be a linear space over $\Re$. If x, y are distinct points of X, the set $\lambda x + (1-\lambda)y, 0 \leq \lambda \leq 1$.
Let;

$f_1 = \Lambda - \beta S(t)I(t) - (\tau + \omega)S(t) + TB(t) - \mu S(t)$

$f_2 = \beta S(t)I(t) - (c + \eta + \mu)E(t)$

$f_3 = \tau S(t) + (c + \eta)E(t) - (\varepsilon + \delta + r + \mu)I(t)$

$f_4 = \omega S(t) + (r + \varepsilon)I(t) - \mu R(t)$

$f_5 = -(T + \mu)B(t)$

Then,

$$\left.\begin{array}{l} |\frac{df_1}{dS}| = |\beta + (\tau+\omega) + \mu| < \infty, \quad |\frac{df_1}{dE}| = |0| < \infty, \quad |\frac{df_1}{dI}| = |\beta| < \infty, |\frac{df_1}{dR}| = |0| < \infty, \\ |\frac{df_1}{dB}| = |T| < \infty \\ |\frac{df_2}{dS}| = |\beta| < \infty, \quad |\frac{df_2}{dE}| = |c + \eta + \mu| < \infty, \quad |\frac{df_2}{dI}| = |0| < \infty, \quad |\frac{df_2}{dR}| = |0| < \infty, \\ \\ |\frac{df_2}{dB}| = |0| < \infty \\ |\frac{df_3}{dS}| = |\tau| < \infty, \quad |\frac{df_3}{dE}| = |c + \eta| < \infty, |\frac{df_3}{dI}| = |(\varepsilon + \delta + r + \mu)| < \infty, \quad |\frac{df_3}{dR}| = |0| < \infty, \\ \\ |\frac{df_3}{dB}| = |0| < \infty \\ |\frac{df_4}{dS}| = |\omega| < \infty, \quad |\frac{df_4}{dE}| = |0| < \infty, \quad |\frac{df_4}{dI}| = |r + \varepsilon| < \infty, \quad |\frac{df_4}{dR}| = |\mu| < \infty, \\ \\ |\frac{df_4}{dB}| = |0| < \infty \\ |\frac{df_5}{dS}| = |0| < \infty, \quad |\frac{df_5}{dE}| = |0| < \infty, \quad |\frac{df_5}{dI}| = |0| < \infty, \quad |\frac{df_5}{dR}| = |0| < \infty, \\ \\ |\frac{df_5}{dB}| = |T + \mu| < \infty \end{array}\right\}$$

The bounded solution of the model exist in all the compartments respectively, therefore is well-posed.

3.3. Disease Free Equilibrium

From the above system of equations, at equilibrium when no outbreak of cholera is observed in the total population, $I(t) = 0$

$\frac{dS}{dt} = \frac{dE}{dt} = \frac{dI}{dt} = \frac{dR}{dt} = \frac{dB}{dt} = 0$

$0 = \Lambda - \beta S(t)I(t) - (\tau + \omega)S(t) + TB(t) - \mu S(t) \quad (i)$

$0 = \beta S(t)I(t) - (c + \eta + \mu)E(t) \quad (ii)$

$0 = \tau S(t) + (c + \eta)E(t) - (\varepsilon + \delta + r + \mu)I(t) \quad (iii)$

$0 = \omega S(t) + (r + \varepsilon)I(t) - \mu R(t) \quad (iv)$

$0 = -(T + \mu)B(t) \quad (v)$

From equations obtained above (v), $0 = -(T + \mu)B(t), B = 0$
From (iii)
$0 = \beta S(t)I(t) - (c + \eta + \mu)E(t), E = 0$
Also from (i)
$0 = \Lambda - \beta S(t)I(t) - (\tau + \omega)S(t) + TB(t) - \mu S(t), S = \frac{\Lambda}{(r+\omega+\mu)}$
it is obtained from (iv)
$0 = \omega S(t) + (r + \varepsilon)I(t) - \mu R(t), R = \frac{\Lambda\omega}{\mu(r+\omega+\mu)}$
Hence, the disease free equilibrium, DFE= $(S_o, E_o, I_o, R_o, B_o)$ where $S_o \neq 0$ as $I = 0$

$$DFE = \left\{ S_o = \frac{\Lambda}{(r+\omega+\mu)}, E = 0, I = 0, R = \frac{\Lambda\omega}{\mu(r+\omega+\mu)}, B = 0 \right\}$$

3.4. Endemic Equilibrium Point

Let $E_e = (S^*, E^*, I^*, R^*, B^*)$ as Endemic equilibrium where $I \neq 0$. Consider the system of equation 2.1 at equilibrium point as:

$0 = \Lambda - \beta S^*(t)I^*(t) - (\tau + \omega)S^*(t) + TB^*(t) - \mu S^*(t) \quad (i)$

$0 = \beta S^*(t)I^*(t) - (c + \eta + \mu)E^*(t) \quad (ii)$

$0 = \tau S^*(t) + (c + \eta)E^*(t) - (\varepsilon + \delta + r + \mu)I^*(t) \quad (iii)$

$0 = \omega S^*(t) + (r + \varepsilon)I^*(t) - \mu R^*(t) \quad (iv)$

$0 = -(T + \mu)B^*(t) \quad (v)$

$$S^* = \frac{\Lambda}{\beta I^* + (\tau + \omega) + \mu}$$

from (iv),$0 = \omega S^*(t) + (r + \varepsilon)I^*(t) - \mu R^*(t)$

$$R^* = \frac{\omega S^* + (r + \omega)I^*}{\mu}$$

From (iii)

$0 = \tau S^*(t) + (c + \eta)E^*(t) - (\varepsilon + \delta + r + \mu)I^*(t)$

$$I^* = \frac{\tau S^* + (c + \eta)E^*}{(\varepsilon + \delta + \mu + r)}$$

From (ii)
$0 = \beta S^*(t)I^*(t) - (c+\eta+\mu)E^*(t)$

$$E^* = \frac{\beta S^* I^*}{(c+\mu+\eta)}$$

$$B^* = \frac{\beta S^* I^* + (\tau+\omega)S^* + \mu S^*}{T-\Lambda}$$

Hence, $E_e = (S^*, E^*, I^*, R^*, B^*)$ are obtained as:

$$E_e = \Bigg\{ S^* = \frac{\Lambda}{\beta I^* + (\tau+\omega) + \mu}, R^* = \frac{\omega S^* + (r+\omega)I^*}{\mu}, I^* = \frac{\tau S^* + (c+\eta)E^*}{(\varepsilon+\delta+\mu+r)}, E^* = \frac{\beta S^* I^*}{(c+\mu+\eta)},$$
$$B^* = \frac{\beta S^* I^* + (\tau+\omega)S^* + \mu S^*}{T-\Lambda} \Bigg\}.$$

3.5. Basic Reproduction Number (R_o)

The basic reproduction number denoted as R_0 . It is necessary to quantify the probability of new cholera infections resulting from a single carrier or sick person in a population without previous illnesses. We use the next-generation approach to create the system described in System of equation, focusing on the infectious classes E, I, and B. The F and V matrices, which represent the rates of new infections and transitions into and out of the infected compartment, respectively, are computed as part of this methodology. These matrices are obtained using a complex derivation from the equations. There are two disease states but only one way to create a new infection. Hence, exposed, infected enable the cholera spread in compartments of the model which are connected from system of equation 2.1. This denotes the number of secondary infections caused as a result of infected individuals in a population. Where $R_o = F \times V^{-1}$.To Obtain R_o from the the spread of cholera disease, it is deduced using next generation matrix where at equilibrium, non-infected sub-populations are disease-free. The transition and transmission matrices V and F are obtained from the partial derivatives of f and v to (E, I, B) evaluated at the disease-free equilibrium E_1

$$F_i = \left(\frac{\partial f_i(x_i)}{\partial x_j}\right) \qquad V_i = \left(\frac{\partial \nu_i(x_i)}{\partial x_j}\right) \quad i,j = 1,2\ldots 7$$

$$\mathbf{F} = \begin{pmatrix} \beta S(t)I(t) & 0 & 0 \\ \tau S(t) & 0 & 0 \\ 0 & 0 & 0 \end{pmatrix} \qquad \mathbf{V} = \begin{pmatrix} (c+\mu+\eta)E(t) \\ -(c+\eta)E(t) + (\varepsilon+\delta+\mu+r)I(t) \\ (T+\mu)B(t) \end{pmatrix}$$

$$\mathbf{F} = \begin{pmatrix} 0 & \beta S_0 & 0 \\ 0 & 0 & 0 \\ 0 & 0 & 0 \end{pmatrix}$$

$$\mathbf{V} = \begin{pmatrix} (c+\mu+\eta) & 0 & 0 \\ -(c+\eta) & (\varepsilon+\delta+\mu+r) & 0 \\ 0 & 0 & (T+\mu)B \end{pmatrix}$$

$$\mathbf{F} = \begin{pmatrix} 0 & \frac{\beta\Lambda}{(r+\omega+\mu)} & 0 \\ 0 & 0 & 0 \\ 0 & 0 & 0 \end{pmatrix}$$

The determinant and inverse of V is thus

$|V| = (c+\mu+\eta)(\varepsilon+\delta+\mu+r)(T+\mu)$
As it is obtained that

$$V^{-1} = \begin{pmatrix} \frac{1}{(c+\mu+\eta)} & 0 & 0 \\ \frac{-(c+\eta)}{(c+\mu+\eta)(\varepsilon+\delta+\mu+r)} & \frac{1}{(\varepsilon+\delta+\mu+r)} & 0 \\ 0 & 0 & \frac{1}{(T+\mu)} \end{pmatrix}$$

Given that, $R_o = F \times V^{-1}$ denoting the product of the matrices obtained

$$R_o = \begin{pmatrix} 0 & \frac{\beta\Lambda}{(r+\omega+\mu)} & 0 \\ 0 & 0 & 0 \\ 0 & 0 & 0 \end{pmatrix} \begin{pmatrix} \frac{1}{(c+\mu+\eta)} & 0 & 0 \\ \frac{-(c+\eta)}{(c+\mu+\eta)(\varepsilon+\delta+\mu+r)} & \frac{1}{(\varepsilon+\delta+\mu+r)} & 0 \\ 0 & 0 & \frac{1}{(T+\mu)} \end{pmatrix}$$

$$= \begin{pmatrix} -\frac{(c+\eta)\beta\Lambda}{(\mu+r+\omega)(c+r+\eta)(\varepsilon+\delta+r+\mu)} & \frac{\beta\Lambda}{(\varsigma+\delta+r+\mu)(\mu+r+\omega)} & 0 \\ \frac{\tau\beta\Lambda}{(c+r+\eta)(\mu+r+\omega)} & 0 & 0 \\ 0 & 0 & 0 \end{pmatrix} - \lambda \begin{pmatrix} 1 & 0 & 0 \\ 0 & 1 & 0 \\ 0 & 0 & 1 \end{pmatrix}$$ on the invariant region of

respective eigen-values it is obtained that $\lambda_i \quad i = 1 \ldots 6$ of $\Re^5_+$ such that $\lambda \geq 0$

$$R_o = \frac{\beta\Lambda}{(\varepsilon+\delta+r+\mu)(\mu+r+\omega)} \tag{3.2}$$

3.6. Local Stability of Disease Free Equilibrium

Theorem 2

The disease-free equilibrium of the model for transmission of cholera disease is locally asymptotically stable if $R_o < 1$ and $R_o > 1$ whenever there is persistency in the spread of disease.

Proof:

The local stability of disease-free equilibrium at $S_o = \frac{\beta\Lambda}{(\mu+r+\omega)}$. The Jacobian matrix of the system 2.1 as obtained that $|J_{E_1} - \lambda_i I| = 0 \quad i = 1, 2 \ldots 5$. Thus, the disease-free equilibrium is locally asymptotically stable if the eigenvalues $\lambda_i, i = 1, \ldots, 5$ of the matrix formed satisfies the condition. The stability criterion of disease-free equilibrium, the general Jacobian matrix has been resolved for as;

$$\mathbf{J}_{(\mathbf{E_1})} = \begin{pmatrix} -(\beta I(t) + \mu + (\tau+\omega)) & 0 & -\beta S_0 & 0 & T \\ \beta I(t) & -(c+\eta+\mu) & \beta S_0 & 0 & 0 \\ \tau & (c+\eta) & -(\varepsilon+\delta+\mu+r) & 0 & 0 \\ \omega & 0 & (r+\varepsilon) & -\mu & 0 \\ 0 & 0 & 0 & 0 & -(\mu+T) \end{pmatrix}$$

Then at disease free equilibrium,

$$\begin{pmatrix} -(\tau+\omega+\mu) & 0 & -\frac{\beta\Lambda}{(\mu+r+\omega)} & 0 & 0 \\ 0 & -(c+\eta+\mu) & \frac{\beta\Lambda}{(\mu+r+\omega)} & 0 & 0 \\ \tau & (c+\eta) & -(\varepsilon+\delta+\mu+r) & 0 & 0 \\ \omega & 0 & (r+\varepsilon) & -\mu & 0 \\ 0 & 0 & 0 & 0 & -(T+\mu) \end{pmatrix}$$

$$\begin{vmatrix} -(\tau+\omega+\mu)-\lambda_1 & 0 & -\frac{\beta\Lambda}{(\mu+r+\omega)} & 0 & 0 \\ 0 & -(c+\eta+\mu)-\lambda_2 & \frac{\beta\Lambda}{(\mu+r+\omega)} & 0 & 0 \\ \tau & (c+\eta) & -(\varepsilon+\delta+\mu+r)-\lambda_3 & 0 & 0 \\ \omega & 0 & (r+\varepsilon) & -\mu-\lambda_4 & 0 \\ 0 & 0 & 0 & 0 & -(T+\mu)-\lambda_5 \end{vmatrix} = 0$$

Also,
where $A = -(\varepsilon+\delta+\mu+r)$. Thus it is obtained that, $\lambda = -(\varepsilon+\delta+\mu+r)$
As obtained from the previously examined determinant of respective eigenvalues, $\lambda = -(c+\eta+\mu)$.
Similarly, the last of the eigenvalue is obtained as;

$$\begin{vmatrix} -(\tau+\omega+\mu)-\lambda_1 & 0 & -\frac{\beta\Lambda}{(\mu+r+\omega)} & 0 & 0 \\ 0 & -(c+\eta+\mu)-\lambda_2 & \frac{\beta\Lambda}{(\mu+r+\omega)} & 0 & 0 \\ \tau & (c+\eta) & -(\varepsilon+\delta+\mu+r)-\lambda_3 & 0 & 0 \\ \omega & 0 & (r+\varepsilon) & -\mu-\lambda_4 & 0 \\ 0 & 0 & 0 & 0 & -(T+\mu)-\lambda_5 \end{vmatrix} = 0,$$

$$[-(\tau+\omega+\mu)-\lambda] \begin{vmatrix} -\frac{\beta\Lambda}{(\mu+r+\omega)} & 0 & 0 & & \\ 0 & -(c+\eta+\mu)-\lambda & \frac{\beta\Lambda}{(\mu+r+\omega)} & 0 & 0 \\ \tau & (c+\eta) & -(\varepsilon+\delta+\mu+r)-\lambda & 0 & 0 \\ \omega & 0 & (r+\varepsilon) & -\mu-\lambda & 0 \\ 0 & 0 & 0 & 0 & -(T+\mu)-\lambda \end{vmatrix} = 0$$

Lastly, from the Jacobian matrix earlier stated,[$\lambda = -(\tau+\omega+\mu)$, respectively;

$$\left.\begin{aligned} \lambda_1 &= -(\tau+\omega+\mu) < 0 \\ \lambda_2 &= -(c+\mu+\eta) < 0 \\ \lambda_3 &= -(\varepsilon+\delta+r+\mu) < 0 \\ \lambda_4 &= -\mu < 0 \\ \lambda_5 &= -(T+\mu) < 0 \end{aligned}\right\}$$

Hence, they are negatively invariant in the region $\Re^5_+$, therefore they are locally asymptotically stable.

3.7. Local Stability of Endemic Equilibrium

Theorem 3

Suppose $X = x_n$ is a space of sequence of real number and we define

$$d(x,y) = \left(\sum_{i=1}^{n} \mid x_i \mid^p \right)^{\frac{1}{p}}, \quad p \geq 1$$

X with the metric is called ξ_n^p space. If $\sum_{i=1}^{\infty} \mid x \mid^p < \infty$ or absolutely convergent and $d(x,y) = \left(\sum_{i=1}^{\infty} \mid x_i - y_i \mid^p \right)^{\frac{1}{p}}$, then X with this metric is called an ξ^p space. It can be checked that for each n;

Proof:

$$0 \leq x_1^2 + x_2^2 + x_3^2 + \ldots + x_n^2 \leq (\mid x_1 \mid + \mid x_2 \mid + \mid x_3 \mid + \ldots + \mid x_n \mid)^2$$

This will result to;

$$x_1^2 + x_2^2 \leq (\mid x_1 \mid + \mid x_2 \mid)^2$$

Therefore,

$$0 \leq (x_1^2 + x_2^2 + x_3^2 + \ldots + x_n^2)^{\frac{1}{2}} \leq \mid x_1 \mid + \mid x_2 \mid + \mid x_3 \mid + \ldots + \mid x_n \mid$$

If $\sum_{n=1}^{\infty} \mid x_n \mid$ converges, that is, $\sum_{n=1}^{\infty} \mid x_n \mid$ is absolutely convergent, then

$$0 \leq (x_1^2 + x_2^2 + x_3^2 + \ldots + x_n^2)^{\frac{1}{2}} \leq \mid x_1 \mid + \mid x_2 \mid + \mid x_3 \mid + \ldots + \mid x_n \mid = \sum_{n=1}^{\infty} \mid x_n \mid < \infty$$

Therefore,

$$0 \leq s_n = x_1^2 + x_2^2 + x_3^2 + \ldots + x_n^2 \leq \left[\sum_{n=1}^{\infty} \mid x_n \mid \right]^2 < \infty$$

The sequence x_n is monotone increasing and bounded above, it therefore converges. Thus $\sum_{n=1}^{\infty} x_n^2$ converges if $\sum_{n=1}^{\infty} x_n$ converges absolutely i.e if $x_n \in \xi^1$, then $x_n \in \xi^2$ where $\xi^1 \leq \xi^2$.
In case of ξ^1 denote the set of all sequences x_n of real numbers such that $\sum_{n=1}^{\infty} x_n$ is convergent absolutely i.e $\sum_{n=1}^{\infty} \mid x_n \mid < \infty$, whereas ξ^2 denote the set of all sequence x_n of real numbers such that $\sum_{n=1}^{\infty} x_n^2 < \infty$ converges. From the preceding, $x_n \in \xi^1 \longleftrightarrow x_n \in \xi^2$ i.e $\xi^1 \subseteq \xi^2$. Further, if $x_n = \frac{1}{n^{\frac{3}{4}}}$, then $\sum_{n=1}^{\infty} \mid x_n \mid$ diverges, and thus $x_n \notin \xi^1$. But $\sum_{n=1}^{\infty} x_n^2 = \sum_{n=1}^{\infty} \frac{1}{n^{\frac{3}{4}}}$ converges, implying that $x_n \in \xi^2$. We conclude then that $\xi^2 \subseteq \xi^1$ and thus $\xi^1 \neq \xi^2$. If x_n, y_n are sequences of real numbers, then

$$\sum_{i=1}^{n} (x_i = y_i)^2 \leq \sum_{i=1}^{n} x_i^2 + \sum_{i=1}^{n} y_i^2 + 2 \left[\sum_{i=1}^{n} x_i^2 \right]^{\frac{1}{2}} \left[\sum_{i=1}^{n} y_i^2 \right]^{\frac{1}{2}}$$

Therefore if $\sum_{i=1}^{\infty} x_i^2 < \infty$ and $\sum_{i=1}^{\infty} y_i^2 < \infty$ then $\sum_{i=1}^{\infty} (x_i - y_i)^2 < \infty$ for all n. The monotone increasing sequence $\left[\sum_{i=1}^{\infty} (x_i - y_i)^2 \right]$ is then bounded above and hence converges i.e $\sum_{i=1}^{\infty} (x_i - y_i)^2 < \infty$. Thus $(x_n - y_n) \in \xi^2$ if x_n, y_n are in ξ^2. The endemic equilibrium of the model outlining the transmission of diphtheria diseases is locally asymptotically stable if $R_o < 1$ and unstable otherwise.
Let $S = p + S^*, E = q + E^*, I = r + I^*, R = a + R^*, B = b + B^*$
By linearizing each state variable of the model formulation, it is obtained that,

$$\frac{dp}{dt} = \Lambda - \beta(p + S^*)(r + I^*) - (\tau + \omega)(p + S^*) + T(b + B^*) - \mu(p + S^*)$$

$$\frac{dq}{dt} = \beta(p + S^*)(r + I^*) - (c + \eta + \mu)(q + E^*)$$

$$\frac{dr}{dt} = \tau(p + S^*) + (c + \eta)(q + E^*) - (\varepsilon + \delta + r + \mu)(r + I^*)$$

$$\frac{da}{dt} = \omega(p + S^*) + (r + \varepsilon)(r + I^*) - \mu(a + R^*)$$

$$\frac{db}{dt} = -(T + \mu)(b + B^*)$$

Hence,

$$\frac{dp}{dt} = -(\beta pr + \tau + \omega + \mu) + Tb + higher - order + non - linear + \dots$$
$$\frac{dq}{dt} = (\beta pr) - (c + \mu + \eta)q + higher - order + non - linear + \dots$$
$$\frac{dr}{dt} = \tau p + (c + \eta)q - (\varepsilon + \delta + r + \mu)r + higher - order + non - linear + \dots$$
$$\frac{da}{dt} = \omega p + (r + \varepsilon)r - \mu a + higher - order + non - linear + \dots$$
$$\frac{db}{dt} = -(T + \mu)b + higher - order + non - linear + \dots$$

The Jacobian matrix of the system

$$\mathbf{J}_{(\mathbf{E}^*)} = \begin{pmatrix} -(\beta r + \tau + \omega + \mu) & 0 & -\beta p & 0 & T \\ \beta r & -(c + \mu + \eta) & \beta p & 0 & 0 \\ \tau & (c + \eta) & -(\varepsilon + \delta + \mu + r) & 0 & 0 \\ \omega & 0 & (\varepsilon + r) & -\mu & 0 \\ 0 & 0 & 0 & 0 & -(T + \mu) \end{pmatrix}$$

From the characteristic equation of $|J_(E^*) - \lambda I| = 0$

$$\begin{vmatrix} a - \lambda & 0 & -\beta p & 0 & T \\ \beta r & b - \lambda & \beta p & 0 & 0 \\ \tau & (c + \eta) & c - \lambda & 0 & 0 \\ \omega & 0 & (\varepsilon + r) & d - \lambda & 0 \\ 0 & 0 & 0 & 0 & e - \lambda \end{vmatrix} = 0$$

It is respectively obtained that the eigen-values become

$$\Big\{ a - \lambda)(b - \lambda)(c - \lambda)(d - \lambda)(e - \lambda) = 0 \Big\}$$

where a =$-(\beta r + \tau + \omega + \mu)$, b = $-(c + \mu + \eta)$, c = $-(\varepsilon + \delta + \mu + r)$, d = $-\mu$ and e = $-(T + \mu)$ Then we have,

$$(a - \lambda)(b - \lambda)(c - \lambda)(d - \lambda)(e - \lambda) = 0$$

Hence, the trace of $J_{E_e} < 0$. Thus, the Jacobian matrix $J_{E_e} < 0$ has eigenvalues that contain negative real roots parts. Therefore, we conclude that the endemic equilibrium point is locally asymptotically stable. Therefore, they are locally asymptotically stable as $R_0 < 1$.

3.8. Global Stability of Disease Free Equilibrium

Considering the use of the Lyapunov algorithm for the system of equation 2.1, which is rapidly tilting to the variance of zero neighborhood is said to be asymptotically stable as $t > 0$. Hence, taken $\psi(t, S, E, I, R, B) = C_1 I_1 + C_2 I_2 + C_3 I_3$

$$\frac{d\psi}{dt} = C_1 I_1' + C_2 I_2' + C_3 I_3'$$

$$\frac{d\psi}{dt} = C_1 \Big(\beta S_0 I_2 - (c + \eta + \mu) I_1 \Big) + C_2 \Big(\tau S_0 + (c + \eta) I_1 - (\varepsilon + \delta + r + \mu) I_2 \Big) + C_3 \Big(- (T + \mu) I_3 \Big)$$

$\frac{d\psi}{dt} \leq [C_2(c+\eta)I_1 - C_1(c+\eta+\mu)I_1] + [C_1\beta S_0 I_2 - C_2(\varepsilon+\delta+\mu+r)I_2] + C_2\tau S_0 - C_3(\tau+\mu)I_3$

$\frac{d\psi}{dt} \leq [C_2(c+\eta) - C_1(c+\eta+\mu)]I_1 + [C_1\beta S_0 - C_2(\varepsilon+\delta+\mu+r)]I_2$

at $S_0 = \frac{\Lambda}{(\tau+\omega+\mu)}, C_1 = \frac{1}{(c+\eta+\mu)}, C_2 = \frac{\beta\Lambda}{(c+\eta+\mu)(\varepsilon+\delta+\mu+r)(\tau+\omega+\mu)}$

$\frac{d\psi}{dt} \leq \left(\frac{\beta\Lambda(c+\eta)}{(c+\eta+\mu)(\varepsilon+\delta+\mu+r)(\tau+\omega+\mu)} - \frac{(c+\eta+\mu)}{(c+\eta+\mu)}\right) + \left(\frac{\beta\Lambda}{(\tau+\omega+\mu)(c+\eta+\mu)} - \frac{\beta\Lambda(\varepsilon+\delta+\mu+r)}{(\varepsilon+\delta+\mu+r)(\tau+\omega+\mu)(c+\eta+\mu)}\right)$

$\frac{d\psi}{dt} \leq \frac{(c+\eta+\mu)}{(c+\eta)}\left\{\frac{\beta\Lambda}{(\varepsilon+\delta+\mu+r)(\tau+\omega+\mu)} - 1\right\}$

$$\frac{d\psi}{dt} \leq \Gamma(R_0 - 1)$$

It is crucial to keep in mind that when at $\frac{d\psi}{dt} = 0$ and $\Gamma = \frac{(c+\eta+\mu)}{(c+\eta)}$. Equation 2.1 can be substituted to find that, according to LaSalle's invariance principle, is globally asymptotically stable whenever $R_0 > 1$ It is crucial to keep in mind that when at $\frac{d\psi}{dt} = 0$. Equation 2.1 can be substituted to find that, according to LaSalle's invariance principle, is globally asymptotically stable whenever $R_0 > 1$

3.9. Global Stability of Endemic Equilibrium

Theorem 4

The model of has no periodic orbits Dulac's criterion states that if $P(x, y)$ is continuously differentiable and $\nabla \cdot (P\mathbf{F}) \neq 0$, no limit cycles exist in $\mathbf{F}$'s domain.

Proof:

Employing the Dulac's criterion on the sub-compartments of the model formulation it is obtained that
Let $X = (S, E, I, R, B)$. Define the Dulac's function as $G = \frac{1}{SE}$

$$\begin{aligned} G\frac{dS}{dt} &= \frac{1}{SE}\left\{\Lambda - \beta S(t)I(t) - (\tau+\omega)S(t) + TB(t) - \mu S(t)S\right\} \\ &= \frac{\Lambda}{SE} - \frac{(\tau+\omega)+\beta I+\mu}{E} + \frac{TB}{SE} \end{aligned}$$

$$\begin{aligned} G\frac{dE}{dt} &= \frac{1}{SE}\left\{\beta S(t)I(t) - (c+\eta+\mu)E(t)\right\} \\ &= \frac{\beta I}{E} - \frac{(c+\eta+\mu)}{S} \end{aligned}$$

$$\begin{aligned} G\frac{dI}{dt} &= \frac{1}{SE}\left\{\tau S(t) + (c+\eta)E(t) - (\varepsilon+\delta+r+\mu)I(t)\right\} \\ &= \frac{\tau}{E} + \frac{(c+\eta)}{S} - \frac{(\varepsilon+\delta+r+\mu)I}{SE} \end{aligned}$$

$$\begin{aligned} G\frac{dR}{dt} &= \frac{1}{SE}\left\{\omega S(t) + (r+\varepsilon)I(t) - \mu R(t)\right\} \\ &= \frac{\omega}{E} + \frac{(r+\varepsilon)I}{SE} - \frac{\mu R}{SE} \end{aligned}$$

$$G\frac{dB}{dt} = \frac{1}{SE}\left\{-(T+\mu)B(t)\right\}$$
$$= \frac{-(T+\mu)B}{SE}$$

$\frac{d(GX)}{dt}$ is obtained as follows:

$$\frac{d(GX)}{dt} = \frac{\partial}{\partial S}\left\{G\frac{dS}{dt}\right\} + \frac{\partial}{\partial E}\left\{G\frac{dE}{dt}\right\} + \frac{\partial}{\partial I}\left\{G\frac{dI}{dt}\right\} + \frac{\partial}{\partial R}\left\{G\frac{dR}{dt}\right\}\left\{G\frac{dB}{dt}\right\}$$

$$\begin{aligned}\frac{d(GX)}{dt} &= \frac{\partial}{\partial S}\left\{\frac{\Lambda}{SE} - \frac{(\tau+\omega)+\beta I+\mu}{E} + \frac{TB}{SE}\right\} + \frac{\partial}{\partial E}\left\{\frac{\beta I}{E} - \frac{(c+\eta+\mu)}{S}\right\} \\ &+ \frac{\partial}{\partial I}\left\{\frac{\tau}{E} + \frac{(c+\eta)}{S} - \frac{(\varepsilon+\delta+r+\mu)I}{SE}\right\} \\ &+ \frac{\partial}{\partial R}\left\{\frac{\omega}{E} + \frac{(r+\varepsilon)I}{SE} - \frac{\mu R}{SE}\right\} + \frac{\partial}{\partial B}\left\{\frac{-(T+\mu)B}{SE}\right\}\end{aligned}$$

$$\frac{d(GX)}{dt} = \left\{-\frac{\mu}{SE}\right\} + \left\{-\frac{(\omega+\mu+\tau)}{SE}\right\} + \left\{-\frac{(c+\eta+\mu)}{SE}\right\} + \left\{-\frac{(\varepsilon+\delta+r+\mu)}{SE}\right\} + \left\{-\frac{\mu}{SE}\right\}$$

$$\frac{d(GX)}{dt} = -\left\{\frac{\mu}{SE} + \frac{(\mu+\tau)}{SE} + \frac{(c+\mu+\omega)}{SE} + \frac{\mu}{SE}\right\}$$

$$\frac{d(GX)}{dt} = -\left\{\frac{2\mu+(\mu+\tau)+(c+\mu+\eta)}{SE}\right\} < 0$$

This implies that the system has no closed orbit. Epidemiologically, the non-existence of a periodic orbit implies that there are fluctuations in the number of infections, which makes it difficult to allocate resources for the control of the disease.

3.10. Sensitivity Analysis

The test for the sensitivity of R_o is to all the parameters in R_0. The normalized forward sensitivity index is defined as shown below

$$\frac{\partial R_o}{\partial P} = \frac{\partial R_o}{\partial P} \times \frac{P}{\partial R_o}$$

Hence,

$$\frac{\partial R_o}{\partial \Lambda} \times \frac{\Lambda}{\partial R_o} = 1.000000$$
$$\frac{\partial R_o}{\partial \omega} \times \frac{\omega}{\partial R_o} = 1.000000$$
$$\frac{\partial R_o}{\partial \beta} \times \frac{\beta}{\partial R_o} = 1.0002101$$
$$\frac{\partial R_o}{\partial \delta} \times \frac{\delta}{\partial R_o} = 1.002190$$
$$\frac{\partial R_o}{\partial r} \times \frac{r}{\partial R_o} = -1.0004200$$
$$\frac{\partial R_o}{\partial \mu} \times \frac{\mu}{\partial R_o} = -1.0001210$$
$$\frac{\partial R_o}{\partial \varepsilon} \times \frac{\varepsilon}{\partial R_o} = 1.101210$$

Table 3.2: Sensitivity Analysis and Indices of the Disease Threshold

Parameters	Indices
Λ	1.000000
ω	1.000000
β	1.0002101
δ	1.002190
r	1.0004200
μ	-1.0001210
τ	1.101210

respectively on each of the sensitive parameters of R_0, result obtained as depicted below. Table 3.2 shows that the sensitivity indices of $\beta, \omega, \varepsilon$ are positive, while μ is negative. As the sensitivity indices depend on the values of the other parameters, changes in those values will affect the sensitivity indices. Based on the table, we can conclude that parameters β and ε are the most sensitive to the basic reproduction number R_0 in equation 3.2 of the cholera model. Specifically, increasing the value of ε will result in a 78.68% increase in R_0, while increasing the value of τ will lead to a 62.64%decrease in R_0.

4. Numerical simulation

In our pursuit of numerically simulating the mathematical model, we aim to offer an approximate solution through the application of the homotopy perturbation method. This choice is motivated by the absence of an exact solution associated with the model. The forthcoming sections will delve into the analysis of the homotopy perturbation method, elucidating its application and implications in our quest for a solution.

$$\Delta(\alpha) = \kappa(\tau) \quad \tau \in \lambda$$

Subject to the boundary condition

$$\Psi(\alpha, \alpha_n) = 0 \quad \tau \in \prod$$

Operator Δ represents the differential operator, Ψ denotes the boundary operator, $\kappa(\tau)$ is an analytic function, Φ is a defined domain bounded by $\prod$, and $\alpha_n$is a normal vector derivative drawn externally from Φ. Thus we can separate the operator $\Delta(\alpha)$ into two:

$$\Delta(\alpha) = L_T(\alpha) + N_T(\alpha)$$

The operator $L_{T(\alpha)}, N_{T(\alpha)}$ denotes the linear and nonlinear term respectively such that equation implies:

$$L_T(\alpha) + N_T(\alpha) = \kappa(\tau) \quad \tau \in \lambda$$

We can construct a Homotopy so that

$$H(f, p) = (1 - p)[L_T(f) - L_T(\omega_0)] + p[\Delta(f) - \kappa(\tau)] = 0$$

Where p is an embedding parameter which can undergo a deformation process of changing from $[0, 1]$. Equation the below equation is further simplified to obtain:

$$H(f, p) = L_T(f) - L_T(\alpha_0) + p[L_T(\alpha_0)] + p[N_T(\alpha_0) - \kappa(\tau)] = 0$$

as equation $p \to 1$ yields:

$$H(f, 0) = L_T(f) - L_T(\alpha_0) = 0$$

And when $p \to 1$ yields:

$$H(f,1) = \Delta(f) - \kappa(\tau) = 0$$

We can naturally assume the solution as a power series such that

$$f(t) = f_0(t) + pf_1(t) + p^2 f_2(t) + \cdot^n f_n(t)$$

Evaluating the above equations, and comparing coefficients of equal powers of p.The values of $f_0(t), f_1(t), f_2(t)$ are obtained by solving the resulting ordinary differential equations. Thus, the approximate solution is obtained as:

$$f(t) = \lim_{p \to 1} f_n(t) = f_1(t) + f_2(t) + f_3(t) + \cdot$$

To conduct numerical simulation on the mathematical model, we create the following correctional scheme for the model equation.

$$\begin{aligned}
0 = (1-p)\frac{dS}{dt} + p\bigg(\Lambda - \beta SI - (\tau+\omega)S + TB - \mu S\bigg) \\
0 = (1-p)\frac{dE}{dt} + p\bigg(\beta SI - (c+\eta+\mu)E\bigg) \\
0 = (1-p)\frac{dI}{dt} + p\bigg(\tau S + (c+\eta)E - (\varepsilon+\delta+r+\mu)I\bigg) \\
0 = (1-p)\frac{dR}{dt} + p\bigg(\omega S + (r+\varepsilon)I - \mu R\bigg) \\
0 = (1-p)\frac{dB}{dt} = p\bigg(- (T+\mu)B\bigg)
\end{aligned}$$

Simplifying the preceding equation yields:

$$\begin{aligned}
\frac{dS}{dt} = p\bigg(\Lambda - \beta SI - (\tau+\omega)S + TB - \mu S\bigg) \\
\frac{dE}{dt} = p\bigg(\beta SI - (c+\eta+\mu)E\bigg) \\
\frac{dI}{dt} = p\bigg(\tau S + (c+\eta)E - (\varepsilon+\delta+r+\mu)I\bigg) \\
\frac{dR}{dt} = p\bigg(\omega S + (r+\varepsilon)I - \mu R\bigg) \\
\frac{dB}{dt} = p\bigg(- (T+\mu)B\bigg)
\end{aligned}$$

The approximate solution of (4.66) can be assumed as:

$$\left.\begin{aligned}
S(t) = s_0(t) + ps_1(t) + p^2 s_2(t) + \ldots + p^n s_n(t) \\
E(t) = e_0(t) + pe_1(t) + p^2 e_2(t) + \ldots + p^n e_n(t) \\
I(t) = i_0(t) + pi_1(t) + p^2 i_2(t) + \ldots + p^n i_n(t) \\
R(t) = r_0(t) + pr_1(t) + p^2 r_2(t) + \ldots + p^n r_n(t) \\
B(t) = b_0(t) + pb_1(t) + p^2 b_2(t) + \ldots + p^n b_n(t)
\end{aligned}\right\}$$

Evaluating and using the comparing coefficient of p^n

$$p^0: \quad s^*(t)=0, e^*(t)=0, i^*(t)=0, r^*(t)=0, b^*(t)=0.$$

Solving this respectively yields

$$s_0(t)=s_0,\ e_0(t)=e_0,\ i_0(t)=i_0,\ r_0(t)=r_0,\ b_0(t)=b_0$$

Solving the system yields:

$$S_1(t)=\left((1-C)B-\frac{(\beta s_0 i_0)}{\alpha(s_0+i_0)}-\mu s_0+\xi r_0\right)t$$
$$E_1(t)=\left(\frac{(\beta s_0 i_0)}{\alpha(s_0+i_0)}-(\delta+\sigma+\mu)e_0\right)t$$
$$I_1(t)=\left(\sigma e_0-(\gamma+\mu\kappa)i_0\right)t$$
$$R_1(t)=p\left(\gamma i_0+\delta e_0+CB-(\xi+\mu)r_0\right)t$$

Following the iterative scheme, two more iterations are computed and the approximate results are evaluated Such that:

$$S(t)=\sum_{n=0}^{4}s_n(t),\ E(t)=\sum_{n=0}^{4}e_n(t),\ I(t)=\sum_{n=0}^{4}i_n(t),\ R(t)=\sum_{n=0}^{4}r_n(t)$$

The approximate results of each class are evaluated using their respective baseline values in Table 1. We also suggest the following population data set as initial values given by $N=7000, s_0=4500, e_0=2050, i_0=142, r_0=306, b_0=2, \omega=0.2102, \eta=0.2317, \tau=0.31, \delta=0.2, \varepsilon=0.0115, \mu=0.01, c=0.31, r=0.0185$.Thus we obtain the following series of results embedding the parameters whose influence on the dynamics of tuberculosis transmission are to be analyzed.

$$\left.\begin{array}{l} s(t)=1000+\Big\{65.26869000=1.3362000\alpha-1362.924000\alpha^2-37.68c\Big\}t+ \\ \Big\{-8.99856418\alpha^2+5499.838828\alpha^4+152.0510083\alpha^2c-0.0997088160\alpha c \\ +3333.926349+45.98509816c-3.288025569\alpha\Big\}\frac{t^2}{2}-\Big\{11.30828286\alpha^2c^2-66.76103861\alpha^2 \\ -0.003719829888\alpha c^2+40645.08576\alpha^4+935.98111186\alpha^2c+56.12092345c \\ -5.923814565\alpha+302.0838612+36988.74452\alpha^6-84.74264814\alpha\Big\}\frac{t^3}{6} \end{array}\right\}$$

$$\left.\begin{array}{l} e(t)=30+\Big\{-45.6259000+1362.924999\alpha^2-1.336200000\alpha\Big\}t \\ -\Big\{69.3893736738-8.9937246462\alpha^3+5499.85264526\alpha^4+152.0510083\alpha^2c-0.997088160\alpha c \\ +5378.9942632c+0.000049369c-5.2993264526\alpha\Big\}\frac{t^2}{2}+\Big\{11.39847747573\alpha^2-80.284635626\alpha^3 \\ -105.5368264253-0.00327426236247\alpha^3c+0.00371362646\alpha c-105.5223642563 \\ +488942646\alpha^4c+1127236.2534\alpha^5c^3+-1.832655321c+16.318372673\alpha^6c^40.000264626\alpha^4c^2 \\ -164264.42663\alpha^3c^3 \\ -84.74264814\alpha^5\Big\}\frac{t^3}{6} \end{array}\right\}$$

$$
\left.
\begin{aligned}
i(t) = 20 - 50.40320t - \Big\{127.0391180 + 0.681642000\alpha^2 - 0.000668\alpha\Big\}\frac{t^2}{2} \\
-\Big\{ -0.004499362535237\alpha^3 + 320.2193625c\alpha + 2.7499236426237\alpha^2c^2 - 0.07636235457\alpha^2c^4 \\
+427466.2635\alpha^4c^2 + 0.37628636623\alpha^4c^4 - 0.003523556\alpha c^2 - 0.5357235\alpha^5 - 1826.725\alpha^2c^6 \\
+2.3545267 \times 10^{-8}c - 0.004330716805\alpha\Big\}
\end{aligned}
\right\}
$$

$$
\left.
\begin{aligned}
r(t) = 40 + (46.18360 + 37.68c)t - \\
\Big\{250.8099123 + 45.9850488c - 2044.386000c\alpha^2 + 2.004300000\alpha\Big\}\frac{t^2}{2} \\
\Big\{13.49785413\alpha^5 - 8249.759899\alpha^4 + 727.7734324 - 228.0765125\alpha^2c + 0.1495632240\alpha c \\
-10561.77617\alpha^2 + 56.12053936c + 10.38388802\alpha\Big\}\frac{t^3}{6}
\end{aligned}
\right\}
$$

$$
\left.
b(t) = 20 - (0.272635c)t - \Big\{4.723633 + 0.2331c\alpha^3 + 1.833.6c + 2..923663\alpha^2\Big\}\frac{t^2}{4}
\right\}
$$

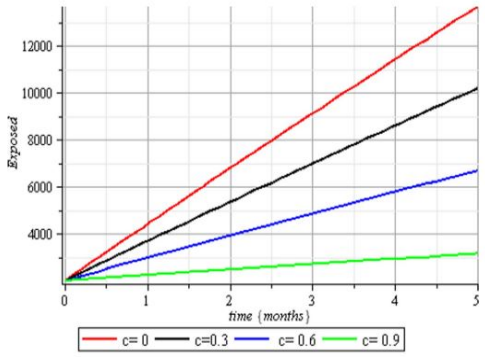

Figure 4.2: Effect of environmental cleanliness on the exposed Population

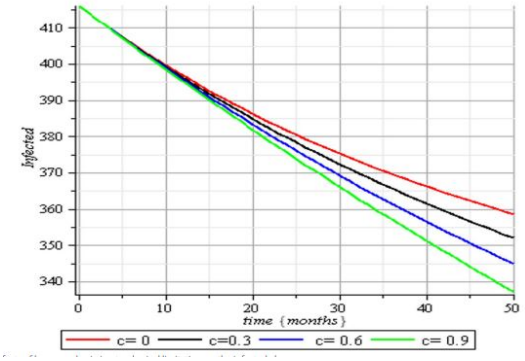

Figure 4.3: Adverse effect of antibiotics on the infected Population

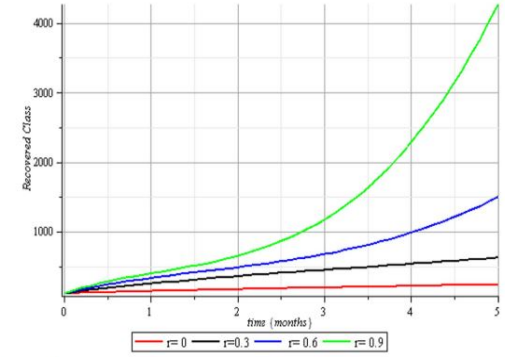

Figure 4.4: Effect of water treatment in the control of cholera transmission in the recovered population

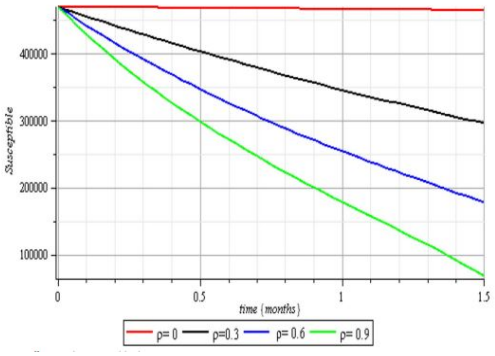

Figure 4.5: Educational program as a control measure on the spread of cholera on the susceptible population

5. Result and interpretation of the graphs

It is obtained that figure 4.2: that environmental cleanliness is a prominent tool in reducing the spread of cholera to the vulnerable population and figure 4.3: Depicts the effect of antibiotics on the infected

population as these bring about a decline in the outbreak of cholera. Figure 4.4: Shows that treatment of water in this region will bring about a drastic measure to the control of cholera as the level of the spread reduces in the population while figure 4.5: The level of educational program sensitization on the set of vulnerable populations reduces as it brings about a rapid spread in cholera outbreak and vice versa.

6. Conclusion

The integration of mathematical modeling with comprehensive control strategies has been instrumental in mitigating cholera spread in remote Nigerian areas during the dry season. Incorporating educational programs, antibiotics, water treatment, and environmental cleanliness into the model has led to significant progress. These initiatives have raised awareness, enabled prompt treatment, ensured access to clean water, and improved sanitation, collectively reducing the impact of cholera outbreaks. Continued collaboration and targeted interventions are crucial for sustaining these efforts and enhancing resilience against cholera in vulnerable populations.

7. Recommendations

This research underscores the critical need for targeted interventions to address cholera outbreaks in remote areas of Nigeria during dry seasons. Based on the findings, it is recommended to implement enhanced water treatment infrastructure, promote sustainable farming practices, and conduct community-specific educational programs. Additionally, policymakers, health practitioners should collaborate with local communities to develop and implement contextually relevant preventive measures. This comprehensive approach will contribute significantly to mitigating cholera spread and building resilience in vulnerable regions.

References

[1] M. Kolawole, A. Oluwarotimi, K. Odeyemi, and A. Popoola, "Analysis of corona-virus mathematical model in asymptomatic and symptomatic cases with vaccine using homotopy perturbation method," *Journal of Applied Computer Science and Mathematics*, vol. 17, no. 1, pp. 20–27, 2023. View online.

[2] M. Bhandari, I. U. Rathnayake, F. Huygens, S. Nguyen, B. Heron, and A. V. Jennison, "Genomic and evolutionary insights into australian toxigenic vibrio cholerae o1 strains," *Microbiology Spectrum*, vol. 11, no. 1, 2023. View online.

[3] A. S. Akanda, A. S. Jutla, and S. Islam, "Dual peak cholera transmission in bengal delta: A hydroclimatological explanation," *Geophysical Research Letters*, vol. 36, no. 19, 2009. View online.

[4] J. C. Caigoy, T. Shimamoto, A. K. Mukhopadhyay, S. Shinoda, and T. Shimamoto, "Sequence polymorphisms in vibrio cholerae hapr affect biofilm formation under aerobic and anaerobic conditions," *Applied and Environmental Microbiology*, vol. 88, no. 17, 2022. View online.

[5] G. Constantin de Magny, R. Murtugudde, M. R. P. Sapiano, A. Nizam, C. W. Brown, A. J. Busalacchi, M. Yunus, G. B. Nair, A. I. Gil, C. F. Lanata, J. Calkins, B. Manna, K. Rajendran, M. K. Bhattacharya, A. Huq, R. B. Sack, and R. R. Colwell, "Environmental signatures associated with cholera epidemics," *Proceedings of the National Academy of Sciences*, vol. 105, no. 46, pp. 17676–17681, 2022. View online.

[6] A. Huq, R. B. Sack, A. Nizam, I. M. Longini, G. B. Nair, A. Ali, J. G. Morris, M. N. H. Khan, A. K. Siddique, M. Yunus, M. J. Albert, D. A. Sack, and R. R. Colwell, "Critical factors influencing the occurrence of vibrio cholerae in the environment of bangladesh," *Applied and Environmental Microbiology*, vol. 71, no. 8, pp. 4645–4654, 2005. View online.

[7] M. K. Kolawole, K. A. Odeyemi, A. O. Oladapo, and K. A. Bashiru, "Dynamical analysis and control strategies for capturing the spread of covid-19," *Tanzania Journal of Science*, vol. 48, no. 3, pp. 680–690, 2022. View online.

[8] M. K. Kolawole, M. O. Olayiwola, H. O. Adekunle, and K. A. Odeyemi, "Conceptual analysis of the combined effects of vaccination, therapeutic actions, and human subjection to physical constraint in reducing the prevalence of covid-19 using the homotopy perturbation method," *Beni-Suef University Journal of Basic and Applied Sciences*, vol. 12, no. 1, 2023. View online.

[9] C. J. Grim, Y. G. Zo, N. A. Hasan, A. Ali, W. B. Chowdhury, A. Islam, M. H. Rashid, M. Alam, J. G. Morris, A. Huq, and R. R. Colwell, "Rna colony blot hybridization method for enumeration of culturable vibrio cholerae and vibrio mimicus bacteria," *Applied and Environmental Microbiology*, vol. 75, no. 17, pp. 5439–5444, 2009. View online.

[10] M. Isikwue, D. Iorver, and S. B. Onoja, "Effect of depth on microbial pollution of shallow wells in makurdi metropoilis, benue state, nigeria," *British Journal of Environment and Climate Change*, vol. 1, no. 3, pp. 66–73, 2011. View online.

[11] J. K. K. Asamoah, F. Nyabadza, M. C. B. Seidu, and H. Dutta, "Mathematical modelling of bacterial meningitis transmission dynamics with control measures," *Computational and Mathematical Methods in Medicine*, vol. 2018, no. 1, 2018. View online.

[12] A. Rinaldo, E. Bertuzzo, L. Mari, L. Righetto, M. Blokesch, M. Gatto, R. Casagrandi, M. Murray, S. M. Vesenbeckh, and I. Rodriguez-Iturbe, "Reassessment of the 2010–2011 haiti cholera outbreak and rainfall-driven multiseason projections," *Proceedings of the National Academy of Sciences*, vol. 109, no. 17, pp. 6602–6607, 2012. View online.

[13] P. Rowlett, "Early careerconnectionswith msor," *MSOR Connections*, vol. 12, no. 2, pp. 17–19, 2012. View online.

[14] S. Y. Suleiman, A. S. Idris, K. Suleiman, A. Abubakar, M. T. Ruma, S. Haladu, I. M. Kaita, and U. B. Ibrahim, "A descriptive epidemiology of cholera outbreak in katsina state, nigeria, 2021," *International Journal of Infectious Diseases*, vol. 116, p. S82, 2022. View online.

[15] S. D. Elek, "The plate virulence test for diphtheria," *Journal of Clinical Pathology*, vol. 2, no. 4, pp. 250–258, 1949. View online.

[16] M. M. EL-Hazmi, "Late-onset prosthetic valve endocarditis caused by nontoxigenic corynebacterium cholera," *The Journal of Infection in Developing Countries*, vol. 9, no. 8, pp. 905–909, 2015. View online.

[17] C. Hailu, G. Fisseha, and A. Gebreyesus, "Determinants of measles vaccination dropout among 12-23 months aged children in pastoralist community of afar, ethiopia," *BMC Infectious Diseases*, vol. 22, no. 1, 2022. View online.

[18] F. P. Havers, P. L. Moro, P. Hunter, S. Hariri, and H. Bernstein, "Use of tetanus toxoid, reduced diphtheria toxoid, and acellular pertussis vaccines: Updated recommendations of the advisory committee on immunization practices-united states, 2019," *Morbidity and Mortality Weekly Report*, vol. 69, no. 3, pp. 77–83, 2020. View online.

[19] F. P. Havers, T. H. Skoff, M. A. Rench, M. Epperson, G. Rajam, J. Schiffer, S. Hariri, L. S. Swaim, C. J. Baker, and C. M. Healy, "Maternal tetanus toxoid, reduced diphtheria toxoid, and acellular pertussis vaccination during pregnancy: Impact on infant anti-pertussis antibody concentrations by maternal pertussis priming series," *Clinical Infectious Diseases*, vol. 76, no. 3, pp. e1087–e1093, 2023. View online.

[20] A. Hoefer, D. Pampaka, S. Herrera-León, S. Peiró, S. Varona, N. López-Perea, J. Masa-Calles, and L. Herrera-León, "Molecular and epidemiological characterization of toxigenic and nontoxigenic corynebacterium diphtheriae, corynebacterium belfantii, corynebacterium rouxii, and corynebacterium ulcerans isolates identified in spain from 2014 to 2019," *Journal of Clinical Microbiology*, vol. 59, no. 3, 2021. View online.

[21] F. Hofmann, "Environmentally and occupationally acquired diseases in adolescents and adulthood: Control of cholera, tetanus, pertussis, and poliomyelitis through regular booster vaccinations european perspective," *Reviews on Environmental Health*, vol. 20, no. 4, pp. 303–317, 2005. View online.

[22] O. Ibrahim, I. Lawal, B. Mohammed, S. Abdullahi, S. Bello, A. Issa, A. Sanda, B. Suleiman, and M. Ibrahim, "Cholera outbreak during covid-19 pandemic in katsina, north-western nigeria: Epidemiological characteristics and predictors of death," *Nigerian Journal of Basic and Clinical Sciences*, vol. 19, no. 1, pp. 59–65, 2022. View online.

[23] V. Keshav, N. Potgieter, and T. Barnard, "Detection of vibrio cholerae o1 in animal stools collected in rural areas of the limpopo province," *Water SA*, vol. 36, no. 2, pp. 167–171, 2010. View online.

[24] E. I. Komarovskaya and V. Perelygyna, "Determination of the specific activity of diphtheria toxoid in combined vaccines by the skin necrosis test method," *Epidemiology and Vaccination*, vol. 22, no. 4, pp. 12–23, 2023. View online.

[25] N. Lawal, S. A. Abdullahi, and D. S. Abolude, "Physicochemical characteristics and fish abundance and diversity of mairua reservoir water, funtua, katsina state, north-western nigeria," *Journal of Applied Sciences and Environmental Management*, vol. 27, no. 1, pp. 125–132, 2023. View online.

[26] B. Liu, "Analysis on the current situation, problems and potential solutions for the chinese precious metals futures market," *BCP Business and Management*, vol. 38, pp. 1239–1244, 2023. View online.

[27] V. G. Melnikov, A. Berger, A. Dangel, and A. Sing, "Lateral flow immunoassay-based laboratory algorithm for rapid diagnosis of diphtheria," *Open Research Europe*, vol. 3:62, 2023. View online.

[28] G. M. Sobamowo, A. A. Yinusa, Z. O. Dere, R. O. Saheed, and R. O. O. Gbadamosi, "Unsteady state heat transfer analysis of a convective-radiative rectangular fin using laplace transform-galerkin weighted residual method," *Journal of Engineering and Thermal Sciences*, vol. 2, no. 2, pp. 84–99, 2022. View online.

[29] A. O. Oladapo, M. O. Olayiwola, K. A. Adedokun, J. A. Adedeji, K. O. Kabiru, and A. O. Yunus, "Optimal control analysis on mathematical model of dynamical transmission of hiv-malaria co-infection," *Journal of Southwest Jiaotong University*, vol. 58, no. 1, 2023. View online.

Format Sitasi IEEE:
Z. O. Dere and A. O. Oladapo, *"Mathematical (Seirb) Model Analysis for Evaluating Cholera Control Strategies in Remote Dry Season Region"*, *Jurnal Diferensial*, vol. 6(2), pp. 148-169, 2024.